

Characterization of the RNA Degradosome of *Pseudoalteromonas haloplanktis*: Conservation of the RNase E-RhlB Interaction in the Gammaproteobacteria[∇]

Soraya Aït-Bara and Agamemnon J. Carpousis*

Laboratoire de Microbiologie et Génétique Moléculaires, UMR 5100, Centre National de la Recherche Scientifique et Université de Toulouse 3, 31062 Toulouse, France

Received 25 May 2010/Accepted 6 August 2010

The degradosome is a multienzyme complex involved in mRNA degradation in *Escherichia coli*. The essential endoribonuclease RNase E contains a large noncatalytic region necessary for protein-protein interactions with other components of the RNA degradosome. Interacting proteins include the DEAD-box RNA helicase RhlB, the glycolytic enzyme enolase, and the exoribonuclease PNPase. *Pseudoalteromonas haloplanktis*, a psychrotolerant gammaproteobacterium distantly related to *E. coli*, encodes homologs of each component of the RNA degradosome. In *P. haloplanktis*, RNase E associates with RhlB and PNPase but not enolase. Plasmids expressing *P. haloplanktis* RNase E (Ph-RNase E) can complement *E. coli* strains lacking *E. coli* RNase E (Ec-RNase E). Ph-RNase E, however, does not confer a growth advantage to *E. coli* at low temperature. Ph-RNase E has a heterologous protein-protein interaction with Ec-RhlB but not with Ec-enolase or Ec-PNPase. The Ph-RNase E binding sites for RhlB and PNPase were mapped by deletion analysis. The PNPase binding site is located at the C-terminal end of Ph-RNase E at the same position as that in Ec-RNase E, but the sequence of the site is not conserved. The sequence of the RhlB binding site in Ph-RNase E is related to the sequence in Ec-RNase E. Together with the heterologous interaction between Ph-RNase E and Ec-RhlB, our results suggest that the underlying structural motif for the RNase E-RhlB interaction is conserved. Since the activity of Ec-RhlB requires its physical interaction with Ec-RNase E, conservation of the underlying structural motif over a large evolutionary distance could be due to constraints involved in the control of RhlB activity.

In the model Gram-negative bacterium *Escherichia coli*, RNase E is an essential RNase involved in RNA processing and mRNA degradation (6, 14, 28). RNase E is a large 1,061-residue protein. Residues 1 to 529 of RNase E correspond to the catalytic domain, which associates to form a tetrameric holoenzyme (3). In *E. coli*, RNase G is a paralog of RNase E, which is 497 residues in length (34, 52, 54). There is a high degree of sequence conservation between the catalytic domains of RNase E and RNase G, and these enzymes have similar catalytic properties. Both enzymes are 5'-end-dependent endoribonucleases with specificity for AU-rich single-strand cleavage sites. The 5'-end dependence involves a site in the catalytic domain that binds 5' monophosphate ends (3, 36). Together, RNase E and RNase G are the founders of a family of bacterial ribonucleases conserved in many, but not all, bacteria (4, 13, 23, 30). A major difference between RNase E and RNase G is the large C-terminal extension of RNase E, which is equal in length to the region corresponding to the catalytic domain.

The noncatalytic region of RNase E, residues 530 to 1061, is mostly natively unstructured (2). However, it contains short regions involved in interactions with phospholipid membranes, RNA, or protein. In some cases, these regions have been shown to form secondary structures involved in the interaction,

and the term “microdomain” has been used to describe these structures (37). “Segment A” of *E. coli* RNase E, corresponding to residues 568 to 582, has recently been shown to form a short amphipathic α -helix that binds to phospholipid membranes *in vitro* and that is necessary for the localization of RNase E to the inner cytoplasmic membrane *in vivo* (25). Residues 604 to 683, known as the arginine-rich RNA binding domain (AR-RBD), binds RNA *in vitro* (38, 51), and it is believed to enhance the activity of RNase E *in vivo* (35, 44). A second short arginine-rich segment (residues 796 to 819), known as AR2 (arginine-rich region 2), is also involved in RNA binding (32). Residues 701 to 1061 form a scaffold for protein-protein interactions with RNA helicase B (RhlB), enolase, and polynucleotide phosphorylase (PNPase) (23, 53). The multienzyme complex comprised of RNase E, RhlB, enolase, and PNPase is known as the RNA degradosome (7, 41, 47). RhlB is a DEAD-box RNA helicase involved in mRNA degradation (24, 47, 53). Enolase is a glycolytic enzyme whose role in RNA metabolism is unclear, although it has been suggested that it might link the mRNA degradation machinery to the control of central intermediary metabolism. PNPase is an exoribonuclease involved in RNA processing and mRNA degradation (12, 19). In the case of enolase and PNPase, the microdomains in the scaffold that are responsible for the protein-protein interactions have been characterized at atomic resolution by X-ray crystallography (8, 43). The microdomain involved in RhlB binding has been localized to a specific region in the scaffold by deletion and point mutation analysis, but its structure has not been elucidated (9, 27, 53).

In addition to the canonical RNA degradosome, a different

* Corresponding author. Mailing address: LMGM, UMR 5100, CNRS-Université Paul Sabatier, 118 route de Narbonne, 31062 Toulouse Cedex 9, France. Phone: 33561335894. Fax: 33561335886. E-mail: carpousis@ibcg.biotoul.fr.

[∇] Published ahead of print on 20 August 2010.

complex containing RNase E, Hfq, and SgrS, a small regulatory RNA, is formed under conditions of phosphosugar stress (42, 55). The formation of the complex with Hfq and SgrS requires the same region of RNase E that is necessary for the formation of the RNA degradosome, and evidence suggests that the degradosome is remodeled because of the new interaction. RraA and RraB, protein factors that downregulate RNase E activity, are also believed to remodel the RNA degradosome, and there is evidence that RNase E can form a "cold shock" RNA degradosome in which CsdA, another DEAD-box RNA helicase, is recruited to the complex (18, 27, 31, 45, 48). The noncatalytic region of RNase E can therefore be viewed as an interaction hub involved in a variety of protein-protein interactions. It has been suggested that remodeling the canonical RNA degradosome in response to environmental changes facilitates the rapid adjustment of the program of gene expression by a posttranscriptional mechanism involving mRNA stability (37).

Authentic homologs of RNase E are found in many bacteria, and in the limited cases studied, these homologs have been found to interact with other enzymes to make RNA degradosome-like complexes (13, 37). The RNase E of the actinobacterium *Streptomyces coelicolor* has been shown to interact with PNPase (30). The RNase E of the photosynthetic alphaproteobacterium *Rhodobacter capsulatus* has been shown to interact with two DEAD-box RNA helicases and the transcription termination factor Rho (20, 21). The RNase E of gammaproteobacterium *Pseudomonas syringae* Lz4W has been shown to interact with a DEAD-box RNA helicase and the exoribonuclease RNase R (46). The composition of the RNase E-based complex thus varies with species, suggesting a specialized role for the RNA degradosome in molecular evolution (37). The variability in composition of the RNA degradosome likely involves changes in the sequences and structure of microdomains in the noncatalytic region of RNase E, although this idea awaits experimental validation.

Pseudoalteromonas haloplanktis TAC125 is a psychrotolerant gammaproteobacterium that was isolated from the Antarctic Ocean (1). Although described as a psychrophilic bacterium, we prefer the term psychrotolerant since it can grow at temperatures ranging from 4°C to 30°C. The genome of *P. haloplanktis* has been completely sequenced (39). Phylogenetic analysis shows that *P. haloplanktis* is a member of the *Alteromonadales*, an order that is separated from the *Enterobacteriales* (*E. coli*) by the *Vibrionales*, *Aeromonadales*, and *Pasteurellales* (17). Interest in *P. haloplanktis* is 2-fold, as follows: industrial applications involving psychrotolerant enzymes and environmental studies involving that adaptation of bacteria to a cold marine niche. Here we have identified and characterized the RNA degradosome of *P. haloplanktis*, showing that it is comprised of RNase E, RhlB, and PNPase but not enolase. The sites in RNase E for protein-protein interactions with RhlB and PNPase were mapped by deletion analysis. Together with a recently published two-hybrid analysis of protein-protein interactions in the RNA degradosome of *Vibrio angustum* S14 (16), this is the first work in which microdomains of RNase E involved in protein-protein interactions have been identified and characterized in a bacterium other than *E. coli*.

MATERIALS AND METHODS

Strains. Strains used in this work are listed in Table 1. *P. haloplanktis* TAC125 was grown at 15°C in TYP broth (16 g/liter yeast extract, 16 g/liter Bacto tryptone, and 15 g/liter NaCl) supplemented with 50 µg/ml ampicillin when necessary.

Plasmids. Plasmids used in this work are listed in Table 1. pSAB11 was constructed by deleting the lactose promoter and operator of pAM238. The gene encoding FLAG-tagged *P. haloplanktis* RNase E (Ph-RNase E) under its own expression signals was constructed by PCR and inserted into pSAB11 to create pSAB15. In pSAB18, the coding sequence of Ph-RNase E was fused at AUG to the *E. coli* RNase E (Ec-RNase E) expression signals. pSAB29 was derived from pSAB18 by deleting the region corresponding to the putative RhlB binding site by inverse PCR.

Conjugation. The shuttle vector pIB3 and *E. coli* strain S17.1 (kindly provided by M. Dreyfus) were used for transconjugation. pIB3 and pSAB17 were mobilized from *E. coli* S17.1 into *P. haloplanktis* TAC125 by conjugation. Aliquots (1 ml) of cultures in logarithmic growth phase were mixed and spotted onto a TYP plate. After 16 h at room temperature, the cells were suspended in 300 µl of TYP broth. Transconjugants were selected at 4°C by plating on TYP plates containing 100 µg/ml ampicillin.

Whole-cell extracts and immunopurification. FLAG-tagged RNase E was immunopurified by a modification of a protocol described previously (42). Cells were grown in 200-ml cultures of LB (*E. coli*) or TYP (*P. haloplanktis*) to an optical density at 600 nm (OD₆₀₀) of 0.6. The cultures were chilled on ice, and all subsequent steps were performed in the cold. The cells were harvested by centrifugation and washed in 10 ml of 50 mM Tris-HCl at pH 8.0 and 5 mM EDTA, except that EDTA was omitted for *P. haloplanktis* since the cells lysed prematurely in its presence. The cell pellets were suspended in 5 ml of IP buffer (20 mM Tris-HCl at pH 8.0, 0.1 M KCl, 5 mM MgCl₂, 10% glycerol, 0.1% Tween 20, 1× Roche EDTA-free protease inhibitor cocktail, 150 µg/ml lysozyme). The cell suspension was subjected to three freeze-thaw steps, sonicated, and centrifuged at 10,000 × g for 1 h at 4°C. The supernatant (1 ml) was incubated with 50 µl of anti-FLAG M2-agarose suspension (Sigma) for 2 h at 4°C with gentle agitation. The mixture was filtered by using a mini-chromatography column (Bio-Rad). The bound proteins were eluted with 50 µl of TBS (50 mM Tris-HCl at pH 7.5 and 0.15 M NaCl) containing 5 µg of FLAG peptide (Sigma). The proteins were separated by sodium dodecyl sulfate-polyacrylamide gel electrophoresis (SDS-PAGE) (7.5%). Western blotting was performed using peroxidase conjugated anti-FLAG antibody (Sigma) and an ECL kit (GE Healthcare).

Purification of RNase E CTH polypeptide and incubation with *P. haloplanktis* cell extracts. The His-tagged RNase E C-terminal half (CTH) polypeptide was expressed using pET15b (Novagen). Briefly, pSAB1 was constructed by ligating the Ph-RNase E coding sequence into pET15b. pSAB20 was constructed by deleting the region corresponding to residues 11 to 528. Thus, the Ph-RNase E CTH polypeptide contains the His tag from pET15b and residues 1 to 10 of Ph-RNase E fused to residues 529 to 1071 of Ph-RNase E. pSAB33, pSAB34, and pSAB35 were derived from pSAB20 by deleting the region corresponding to the last 231, 76, and 37 residues of Ph-RNase E CTH, respectively.

BL21(DE3) was transformed with pSAB20, pSAB33, pSAB34, and pSAB35. Cultures were grown at 30°C and induced at an OD₆₀₀ of 0.4 to 0.5 with 1 mM IPTG (isopropyl-β-D-thiogalactopyranoside). Cells were harvested 3 h after induction by centrifugation at 6,000 rpm at 4°C for 15 min and washed with ice-cold 50 mM Tris-HCl, pH 7.5. The following steps, which were done under denaturing conditions in 8 M urea, were performed at room temperature. A cleared lysate was prepared in buffer B according to the manufacturer's instructions (Qiagen). Approximately 100 µg of overexpressed protein was diluted in buffer B and incubated with 200 µl of Talon metal affinity resin (cobalt; Clontech). The beads were collected in a mini-chromatography column (Bio-Rad) and washed with 1 ml buffer C (Qiagen). The urea was removed by washing with buffer EQ (20 mM Tris-HCl at pH 7.5, 0.1 M KCl, 5 mM MgCl₂, 10% glycerol, 0.1% Tween 20, 0.1 mg/ml bovine serum albumin [BSA], and 1× Roche EDTA-free protease inhibitor cocktail). The column was transferred to 4°C and washed again with cold buffer EQ. Subsequent steps were performed at 4°C. Whole-cell extract (1 ml) from *P. haloplanktis* was added and incubated for 2 h. The column was washed twice with buffer 1 (buffer EQ containing 20 mM imidazole without BSA). Elutions were performed with buffer 2 (buffer 1 containing 300 mM imidazole).

Mass spectrometry. Proteins that copurified with FLAG-tagged Ph-RNase E were identified by mass spectrometry. Bands from SDS-PAGE were excised and sent to the proteomics service of the University of Bordeaux for analysis (Plateforme de Génomique Fonctionnelle Bordeaux, Université Victor Segalen). Coverage ranged from 47% for PNPase to 20% for RhlB.

TABLE 1. Strains and plasmids

Strain/plasmid	Description ^a	Reference/ source
Strains		
<i>P. haloplanktis</i> TAC125	Wild type	1
KSL2000	<i>rne::cat recA::Tn10</i>	31
AC21	MC1061 <i>zce-726::Tn10</i>	8
AC27	MC1061 <i>zce-726::Tn10 rne131</i>	34
SVK438	KSL2000 <i>recA</i> ⁺	V. Khemici
SVK446	KSL2000 <i>recA</i> ⁺ Δ <i>rhlb</i>	V. Khemici
S17.1	RP4 2-Tc::Mu-Km::Tn7 <i>pro res mod1</i>	52
BL21(DE3)	F ⁻ <i>ompT hsdS_B(r_B⁻ m_B⁻) dcm gal λ(DE3)</i>	53
Plasmids		
pAM238	pGB2-derived plasmid	12
pAM- <i>rne</i>	Chromosomal PstI fragment containing the <i>rne</i> gene cloned into pAM238 (pSC101ori, spectinomycin resistance)	56
pVK200	pAM238, Ec-RNase E, C-terminal FLAG	V. Khemici
pET15b-RneCTH	T7 expression of the RNase E CTH with an N-terminal His tag	29
pJB3	Broad-host-range cloning vector, RK2 derivative plasmid	2
pIB3 (shuttle vector)	Fragment 1914 to 2786 of the resident plasmid pMtBL of <i>P. haloplanktis</i> containing the origin of replication was cloned into pJB3	Ivona Bagdiul
pSAB1	pET15b, <i>Ph-rne</i> CDS under the control of T7 expression signals	This work
pSAB11	pAM238, lactose expression signals deleted	This work
pSAB12	pSAB11, <i>Ph-rne</i>	This work
pSAB13	pSAB11, <i>E. coli</i> expression signals fused to <i>Ph-rne</i> CDS	This work
pSAB15	pSAB11, <i>Ph-rne</i> , C-terminal FLAG	This work
pSAB17	pIB3, <i>Ph-rne</i> , C-terminal FLAG	This work
pSAB18	pSAB15, <i>E. coli</i> expression signals fused to <i>Ph-rne</i> CDS	This work
pSAB29	pSAB18, <i>Ph-rne</i> (deletion of HBS)	This work
pSAB20	pSAB1, <i>Ph-rne</i> (deletion of residues 11–528)	This work
pSAB33	pSAB20, <i>Ph-rne</i> CTH (deletion of residues 841–1071)	This work
pSAB34	pSAB20, <i>Ph-rne</i> CTH (deletion of residues 996–1071)	This work
pSAB35	pSAB20, <i>Ph-rne</i> CTH (deletion of residues 1035–1071)	This work

^a CDS, coding sequence.

PONDR and ClustalW. The *P. haloplanktis* RNase E protein sequence was analyzed by the Predictor of Naturally Disordered Regions (PONDR) (Molecular Kinetics, Inc., Indianapolis, IN) (33). Protein sequence alignments were performed on the EMBL-EBI website (<http://www.ebi.ac.uk/Tools/clustalw2/index.html>) using CLUSTALW (10) and the Jalview editor (11).

RESULTS

Prediction of microdomains in the noncatalytic region of Ph-RNase E. The genome of *P. haloplanktis* encodes orthologs of *E. coli* RNase E, RhlB, enolase, and PNPase that are conserved with overall sequence identities ranging from 52% for RNase E to 78% for enolase (data not shown). The score for the N-terminal catalytic domain (residues 1 to 529) of RNase E is 78% identity. No significant sequence conservation was detected between the C-terminal noncatalytic region of *P. haloplanktis* RNase E (Ph-RNase E) and *E. coli* RNase E (Ec-RNase E), a result consistent with previous work demonstrating a high degree of sequence variability in the noncatalytic region, even in closely related bacteria. Experimental work with *E. coli* RNase E has revealed six segments in the noncatalytic region that are involved in interactions with the phospholipid membrane, RNA, or protein (Fig. 1A). The membrane-targeting sequence (MTS) has been shown to interact with phospholipid membranes (25). The arginine-rich RNA binding domain (AR-RBD) and a second arginine-rich region (AR2) have been shown to bind RNA. The helicase binding site (HBS), enolase-binding site (EBS), and PNPase binding

site (PBS) have been shown to bind RhlB, enolase, and PNPase, respectively. Three of these segments overlap with or correspond to regions that have been predicted by PONDR to have the propensity to form secondary structures (Fig. 1A, segments A, C, and D), and experimental results have confirmed these predictions (2, 8, 25, 43). Segment B, which overlaps the AR-RBD, is predicted to have the propensity to form a coiled-coil structure, although there is no experimental evidence supporting this prediction.

We analyzed the protein sequence of Ph-RNase E by PONDR, and the profile shown in Fig. 1B is similar to that shown in results previously obtained with the RNase E of *E. coli* and *Vibrio angustum* S14 (2, 16). For comparison, the profile for Ec-RNase E is shown in Fig. 1A. The conserved N-terminal catalytic domain of Ph-RNase E is predicted to be mostly structured. Segment A in the noncatalytic region, which corresponds to the MTS, is clearly predicted to be structured, consistent with previous work showing that this microdomain is conserved throughout the gammaproteobacteria (25). Three other short segments of predicted structure were detected in the noncatalytic region of Ph-RNase E (Fig. 1B, regions 1 to 3), but by visual inspection and sequence alignment, there is no obvious correspondence to any of the microdomains identified in Ec-RNase E. The only other clearly discernible elements in the noncatalytic region of the Ph-RNase E are the AR-RBD and AR2, which were detected by visual inspection and alignment of the Ec-RNase E and Ph-RNase sequences. In sum-

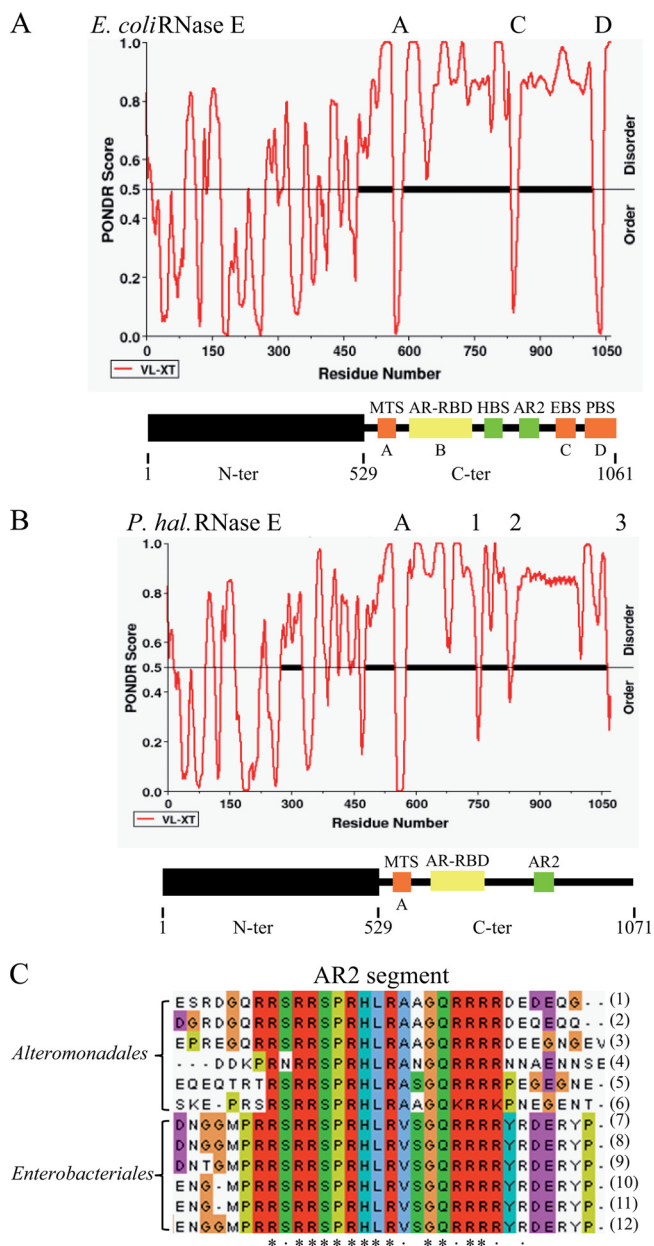


FIG. 1. Primary structure of *P. haloplanktis* RNase E. (A, B) PONDRA analysis for prediction of RISPs (regions of increased structural propensity) and schematic representation of Ec-RNase E (A) and Ph-RNase E (B). RISPs correspond to regions with a score of less than 0.5. The analysis of Ec-RNase E, which has appeared previously (2), is presented to permit direct comparison with Ph-RNase E. In the schematic, the N-terminal catalytic domain is represented as a black box, and the noncatalytic C-terminal region is represented as a line. The noncatalytic region of Ec-RNase E contains six microdomains involved in membrane, RNA, and protein interactions. MTS, membrane targeting sequence; AR-RDB, arginine-rich RNA binding domain; HBS, helicase binding site; AR2, arginine-rich region 2; EBS, enolase binding site; PBS, PNPase binding site. Segments A, C, and D (red) correspond to regions predicted to form secondary structures by PONDRA. Segment B (yellow), which overlaps with the AR-RBD, was predicted to form a coiled-coil structure (see reference 2). Two other microdomains (green) are known to make interactions but do not correspond to regions of predicted secondary structure. (C) Sequence alignment of the AR2 segments of RNase E homologs from the *Alteromonadales* and *Enterobacteriales*. The asterisks indicate strictly conserved resi-

dues; the dots indicate residues that are similar. The homologs used in this alignment correspond to *Shewanella* sp. ANA-3 (1), *Shewanella amazonensis* SB2B (2), *Shewanella* sp. PV-4 (3), *Colwellia psychrerythraea* 34H (4), *Pseudoalteromonas haloplanktis* TAC125 (5), *Pseudoalteromonas tunicata* D2 (6), *Escherichia coli* (7), *Shigella boydii* Sb227 (8), *Salmonella enterica* subsp. *enterica* (9), *Yersinia pestis* Antiqua (10), *Yersinia pseudotuberculosis* IP 31758 (11), and *Erwinia carotovora* subsp. *atroseptica* SCRI1043 (12).

dues; the dots indicate residues that are similar. The homologs used in this alignment correspond to *Shewanella* sp. ANA-3 (1), *Shewanella amazonensis* SB2B (2), *Shewanella* sp. PV-4 (3), *Colwellia psychrerythraea* 34H (4), *Pseudoalteromonas haloplanktis* TAC125 (5), *Pseudoalteromonas tunicata* D2 (6), *Escherichia coli* (7), *Shigella boydii* Sb227 (8), *Salmonella enterica* subsp. *enterica* (9), *Yersinia pestis* Antiqua (10), *Yersinia pseudotuberculosis* IP 31758 (11), and *Erwinia carotovora* subsp. *atroseptica* SCRI1043 (12).

dues; the dots indicate residues that are similar. The homologs used in this alignment correspond to *Shewanella* sp. ANA-3 (1), *Shewanella amazonensis* SB2B (2), *Shewanella* sp. PV-4 (3), *Colwellia psychrerythraea* 34H (4), *Pseudoalteromonas haloplanktis* TAC125 (5), *Pseudoalteromonas tunicata* D2 (6), *Escherichia coli* (7), *Shigella boydii* Sb227 (8), *Salmonella enterica* subsp. *enterica* (9), *Yersinia pestis* Antiqua (10), *Yersinia pseudotuberculosis* IP 31758 (11), and *Erwinia carotovora* subsp. *atroseptica* SCRI1043 (12).

dues; the dots indicate residues that are similar. The homologs used in this alignment correspond to *Shewanella* sp. ANA-3 (1), *Shewanella amazonensis* SB2B (2), *Shewanella* sp. PV-4 (3), *Colwellia psychrerythraea* 34H (4), *Pseudoalteromonas haloplanktis* TAC125 (5), *Pseudoalteromonas tunicata* D2 (6), *Escherichia coli* (7), *Shigella boydii* Sb227 (8), *Salmonella enterica* subsp. *enterica* (9), *Yersinia pestis* Antiqua (10), *Yersinia pseudotuberculosis* IP 31758 (11), and *Erwinia carotovora* subsp. *atroseptica* SCRI1043 (12).

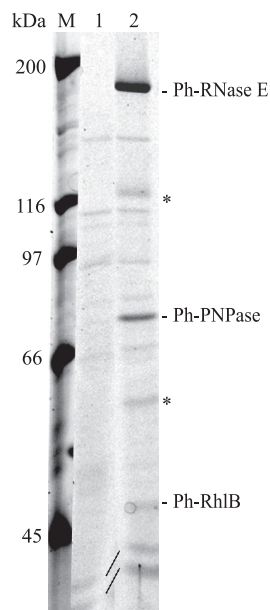


FIG. 2. RNA degradosome of *P. haloplanktis*. SDS-PAGE stained with Sypro orange. Whole-cell extracts were prepared from *P. haloplanktis* conjugated with the empty shuttle vector (pIB3) or the vector encoding FLAG-tagged Ph-RNase E (pSAB17). After absorption to the anti-FLAG agarose beads and being washed, Ph-RNase E was eluted with FLAG peptide. Lane 1, pIB3 (background control); lane 2, pSAB17 (FLAG-tagged Ph-RNase E). M, molecular mass markers. The proteins shown in lane 2 were identified by mass spectrometry. The asterisks indicate proteolytic products of Ph-RNase E.

not shown). Enolase is a highly conserved enzyme, and control experiments showed that our antiserum readily detects Ph-enolase in *P. haloplanktis* whole-cell extracts (data not shown). Taken together, these results show that the Ph-RNase E forms an RNA degradosome containing Ph-PNPase and Ph-RhlB and suggest that Ph-enolase is not tightly associated with Ph-RNase E (see below).

Complementation of *E. coli* strains lacking Ec-RNase E by Ph-RNase E. We wanted to test whether Ph-RNase E could replace the function of Ec-RNase E in *E. coli* and whether the substitution of a mesophilic RNase E by a psychrotolerant RNase E affects the growth of *E. coli* in the cold. We used the KSL2000 strain of *E. coli*, in which the gene encoding RNase E on the chromosome is disrupted (29). Since RNase E is essential, it is supplied in *trans* by pBAD-*rne*, which is a low-copy-number plasmid with the Ec-RNase E coding sequence under the control of the *arabinose* promoter. We transferred the *Ph-rne* gene with the FLAG tag from pSAB17 to pSAB11 to create pSAB15. Both pBAD-*rne* and pSAB15 have the same origin of DNA replication (pSC101) but different antibiotic resistance markers. By transforming the KSL2000 strain with pSAB15 and selecting for spectinomycin, it was possible to displace the pBAD-*rne* plasmid and complement the deletion of Ec-RNase E on the chromosome with *Ph-rne* on the plasmid. However, this strain formed only visible colonies after 6 days of growth at 25°C compared to the control strain complemented with *Ec-rne* (pVK200), which formed visible colonies after 2 days (Fig. 3A). A control experiment using Ph-RNase E without FLAG gave the same result (data not shown). Quan-

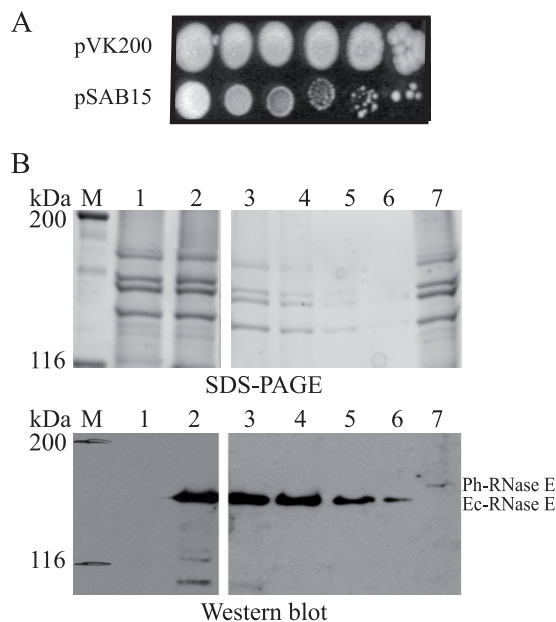


FIG. 3. Complementation of KSL2000 and expression of Ph-RNase E in *E. coli*. (A) Complementation of the KSL2000 strain (disruption of the chromosomal gene encoding Ec-RNase E) by plasmids expressing FLAG-tagged Ec-RNase E (pVK200) or FLAG-tagged Ph-RNase E (pSAB15). Serial dilutions (10-fold) were spotted on LB plates and grown at 25°C for 6 days. (B) SDS-PAGE stained with Sypro orange and Western blotting using anti-FLAG antibodies. Lane 1, pAM-*rne* (Ec-RNase E without FLAG); lane 2, pVK200; and lane 7, pSAB15. M, molecular mass markers. The protein loaded in lane 2 was diluted 4-fold (lane 3), 8-fold (lane 4), 16-fold (lane 5), and 32-fold (lane 6). In the panel showing lanes 1 and 2, the blot was exposed for 30 s, whereas in the panel showing lanes 3 to 7, the blot was exposed for 4 min to permit detection of Ph-RNase E.

tative Western blotting (Fig. 3B), in which a cell extract from the *Ec-rne* control was serially diluted, showed that the amount of Ph-RNase E in the strain complemented with pSAB15 was at least 32-fold lower than the amount of Ec-RNase E in the strain complemented with pVK200 (Fig. 3B, compare lane 7, undiluted Ph-RNase E, to lane 6, 32-fold-diluted Ec-RNase E). Note that in Fig. 3B, the image corresponding to lanes 3 to 7 was the result of a 4-min exposure to permit detection of Ph-RNase E, whereas the panel corresponding to lanes 1 and 2 was the result of a 30-s exposure. We therefore hypothesized that the weak complementation of the KSL2000 strain by pSAB15 might be due to low levels of expression of Ph-RNase E.

Promoters of transcription in *P. haloplanktis* have essentially the same consensus sequence as those in *E. coli* and are therefore expected to act as promoters in *E. coli* (15). The genomic region containing the *Ph-rne* gene used in our experiments contains approximately 700 bp of DNA upstream of the *rne* coding sequence. This region, which includes a 400-bp intergenic spacer and part of an upstream coding sequence, contains signals for transcription and translation, as evidenced by expression of FLAG-tagged Ph-RNase E when the gene carried by pSAB17 was introduced into *P. haloplanktis* by conjugation (Fig. 2). The control of the expression of Ec-RNase E involves a complex system of posttranscriptional autoregulation in which a 361-nucleotide (nt)-long 5' untranslated region

is targeted by RNase E to destabilize the mRNA (22). Taken together, our results suggest that low-level expression is due to a dysfunction in either the transcriptional or posttranscriptional control of the *Ph-rne* gene in *E. coli*.

To express Ph-RNase E at levels comparable to those of Ec-RNase E in the KSL2000 strain, we constructed a hybrid *rne* gene in which the 5' noncoding region of *Ec-rne* was fused to the coding sequence of Ph-RNase E. pSAB18, harboring the *rne* fusion, transformed into KSL2000 exhibited robust complementation at temperatures ranging from 25 to 37°C (Fig. 4A). Western blotting showed that the amount of Ph-RNase E in the strain complemented by pSAB18 is about 50% of the amount of Ec-RNase E in the strain complemented by pVK200 (Fig. 4B and quantification not shown). Taken together, these results suggest that the weak complementation by pSAB18 is due to low levels of expression of Ph-RNase E in *E. coli* when the coding sequence is under the control of the homologous *P. haloplanktis* expression signals. In Fig. 4A, Ph-RNase E failed to complement at 42°C, which is likely due to the thermostability of Ph-RNase E.

It is notable that complementation by Ph-RNase E at 15°C is weak (Fig. 4A). The amount of Ph-RNase E does not change between 30 and 15°C, as shown by Western blotting (Fig. 4B). Therefore, the growth defect at 15°C is not due to small amounts of Ph-RNase E. Since the endoribonuclease activity of Ph-RNase E is expected to be robust at 15°C, relatively poor growth at this temperature suggests that Ph-RNase E fails to provide a noncatalytic function that is necessary for growth in the cold. Moreover, the *E. coli* MC1061 strain harboring the *rne131* mutant lacking the last 477 residues of Ec-RNase E (32) grows slower than the wild-type strain at 15°C, whereas at 30°C, no growth defect was observed (Fig. 4C). Thus, the noncatalytic region of Ec-RNase E appears to have a function at low temperature that is not provided by Ph-RNase E.

Heterologous interaction between Ph-RNase E and Ec-RhlB. Since we were able to complement the KSL2000 strain with FLAG-tagged Ph-RNase E, we decided to check for heterologous interactions with *E. coli* proteins. By following the same strategy described above for the characterization of the RNA degradosome in *P. haloplanktis*, FLAG-tagged Ph-RNase E was purified from *E. coli* whole-cell extracts using anti-FLAG agarose beads. In Fig. 5A, lane 1 contains a negative control showing KSL2000 complemented with pAM-*rne* (harboring Ec-RNase E without FLAG). The three proteins marked with the asterisks are subunits of pyruvate dehydrogenase, an *E. coli* enzyme that adventitiously reacts with the FLAG agarose beads (42). Lane 2 contains a control showing the results from the KSL2000 strain complemented with pVK200 (FLAG-tagged Ec-RNase E). As expected, Ec-PNPase, Ec-RhlB, and Ec-enolase copurify with Ec-RNase E. Lane 3 shows the results from the KSL2000 strain complemented with pSAB18 (FLAG-tagged Ph-RNase E). We detected neither Ec-PNPase nor Ec-enolase. This result was confirmed by Western blotting, which should have been sensitive enough to detect trace amounts of PNPase or enolase (data not shown). The failure to detect enolase in lane 3 of Fig. 5A corroborates the results in Fig. 2, adding support to the suggestion that Ph-RNase E does not tightly associate with enolase. There was, however, in Fig. 2, a protein associated with Ph-RNase E that migrated at 50 kDa with mobility identical to that of Ec-RhlB.

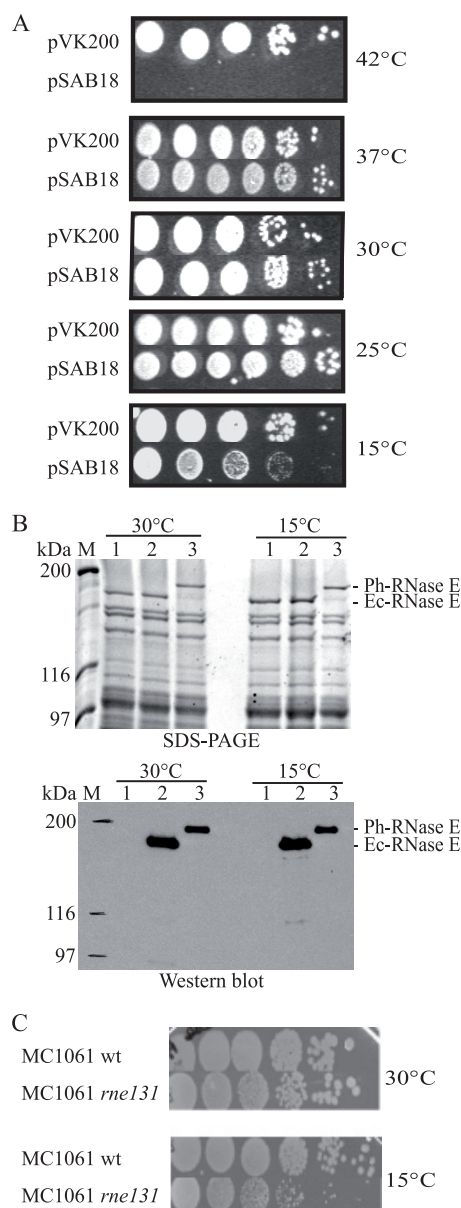


FIG. 4. Complementation of KSL2000, expression of Ph-RNase E at 30 and 15°C, and growth of the MC1061 *rne131* strain at 15°C. (A) Complementation of the KSL2000 strain (the chromosomal gene encoding Ec-RNase E was disrupted) by a plasmid expressing FLAG-tagged Ph-RNase E (pSAB18). Serial dilutions (10-fold) were spotted on LB plates and grown at the indicated temperatures for times ranging from 1 day (37 and 42°C) to 10 days (15°C). (B) SDS-PAGE stained with Sypro orange and Western blotting using anti-FLAG antibodies. Lane 1, KSL2000 complemented with pAM-*rne* (Ec-RNase E without FLAG); lane 2, pVK200 (Ec-RNase E with FLAG); and lane 3, pSAB18 (Ph-RNase E with FLAG). M, molecular mass markers. (C) Growth of MC1061 (wild type [wt], AC21) and the *rne131* derivative (AC27) at 30 and 15°C (10-fold serial dilutions).

This protein was identified as Ec-RhlB by Western blotting (data not shown) and by repeating the experiment using a strain of *E. coli* (SVK446) in which the gene encoding RhlB was disrupted (Fig. 5B). The absence of the band corresponding to Ec-RhlB in lane 2 (Ec-RNase E) and lane 3 (Ph-RNase

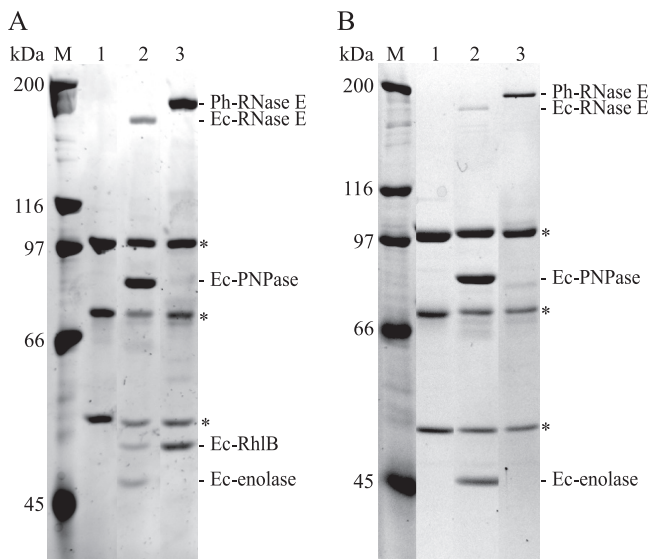


FIG. 5. Ph-RNase E expressed in *E. coli* interacts with Ec-RhlB. SDS-PAGE stained with Sypro orange. (A) Immunopurifications were performed as shown in Fig. 2. Lane 1, KSL2000 complemented with pAM-*rne* (Ec-RNase E without FLAG); lane 2, pVK200 (Ec-RNase E with FLAG); and lane 3, pSAB18 (Ph-RNase E with FLAG). M, molecular mass markers. The asterisks indicate subunits of pyruvate dehydrogenase, which interacts adventitiously with the FLAG antibody. (B) The experiment shown in panel A was repeated using a strain (SVK446) in which the gene encoding RhlB was disrupted.

E) confirms that the protein associated with Ph-RNase E is Ec-RhlB. Taken together, these results show that Ph-RNase E makes a heterologous interaction with Ec-RhlB but not Ec-PNPase or Ec-enolase.

Identification of the RhlB binding site in Ph-RNase E. In order to identify the helicase binding site (HBS) in Ph-RNase E, we aligned the sequences of RNase E homologs from the *Alteromonadales*, the order of bacteria that includes *P. haloplanktis*. We identified a motif located in the same region as the HBS of RNase E homologs from the *Enterobacteriales* that is related by sequence (Fig. 6A). These motifs have in common a core of 13 residues, with 5 positions that are strictly conserved. To test if the motif identified in Ph-RNase E is necessary for RhlB binding, we deleted the corresponding region in pSAB18 to create pSAB29. The deletion corresponds to the boxed sequence in Fig. 6A. Figure 6B shows that the deletion results in the loss of the immunopurification of RhlB with Ph-RNase E (compare lanes 1 and 2). From this result, we conclude that the sequence motif identified in Fig. 5A corresponds to the microdomain necessary for the heterologous protein-protein interaction between Ec-RhlB and Ph-RNase E.

Identification of the PNPase binding site in Ph-RNase E. Using the same approach that led to the identification of the HBS, we failed to identify a sequence motif in the RNase E homologs of the *Alteromonadales* that was related to the PNPase binding site (PBS) of Ec-RNase E. Since the PBS is located in the C-terminal region of Ec-RNase E and since this region in Ph-RNase E is predicted to have the propensity to form secondary structure (Fig. 1B, region 3), we decided to construct a series of nested deletions extending from the C-terminal end into the protein. The protein interaction was tested *in vitro*

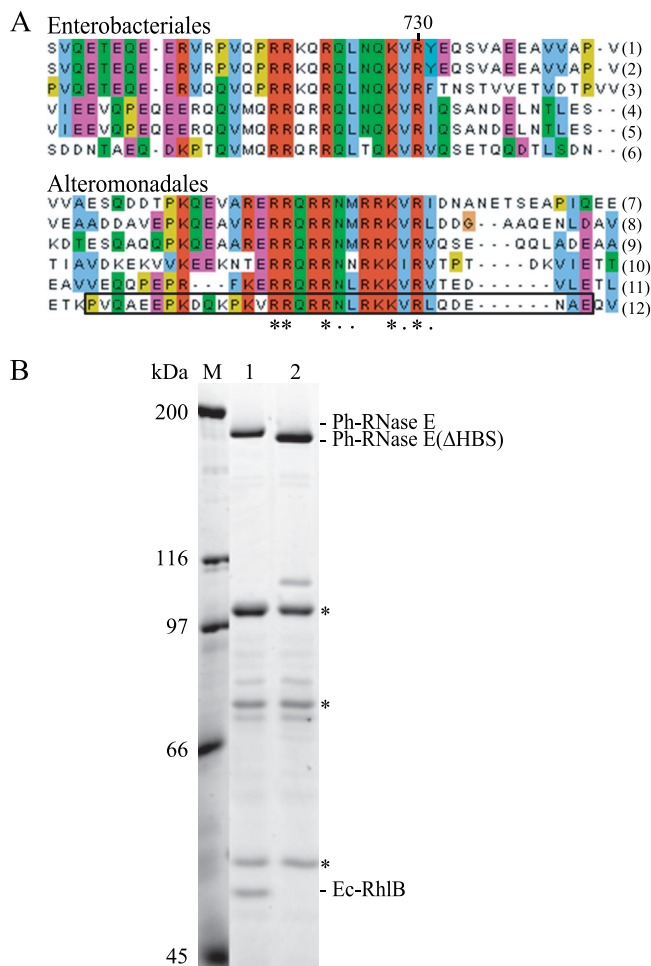


FIG. 6. Identification of the RhlB binding site of Ph-RNase E. (A) Sequence alignment of the HBSs in homologs from the *Enterobacteriales* (top) and the corresponding regions in homologs from the *Alteromonadales* (bottom). The asterisks indicate residues that are conserved; the dots indicate residues that are similar. The homologs used in these alignments correspond to *Escherichia coli* (1), *Shigella boydii* Sb227 (2), *Salmonella enterica* subsp. *enterica* (3), *Yersinia pseudotuberculosis* IP 31758 (4), *Erwinia carotovora* subsp. *atroseptica* SCRI1043 (5), *Yersinia pestis* Antiqua (6), *Shewanella* sp. ANA-3 (7), *Shewanella amazonensis* SB2B (8), *Shewanella* sp. PV-4 (9), *Colwellia psychrerythraea* 34H (10), *Pseudoalteromonas tunicata* D2 (11), and *Pseudoalteromonas haloplanktis* TAC125 (12). The deletion of the region corresponding to the motif identified in Ph-RNase E in pSAB18 to create pSAB29 corresponds to the boxed sequence in the alignment. (B) SDS-PAGE stained with Sypro orange. Immunopurifications were performed as shown in Fig. 2. Lane 1, pSAB18 (Ph-RNase E with FLAG); lane 2, pSAB29, which expresses a variant of Ph-RNase E deleted from residues 684 to 716 (boxed in panel A, last line). M, molecular mass markers. The asterisks correspond to the subunits of pyruvate dehydrogenase, which interacts adventitiously with the FLAG antibody.

using an N-terminal His-tagged derivative corresponding to the noncatalytic C-terminal half (CTH) of Ph-RNase E (Fig. 7A). We showed previously that the Ec-CTH interacts with Ec-PNPase *in vitro* to form a complex that can be purified using a His tag (27). In the experiment performed here, the Ph-CTH was overexpressed in *E. coli* and purified by affinity chromatography. The resin with the bound Ph-CTH was then incubated with a whole-cell extract prepared from *P. haloplanktis*,

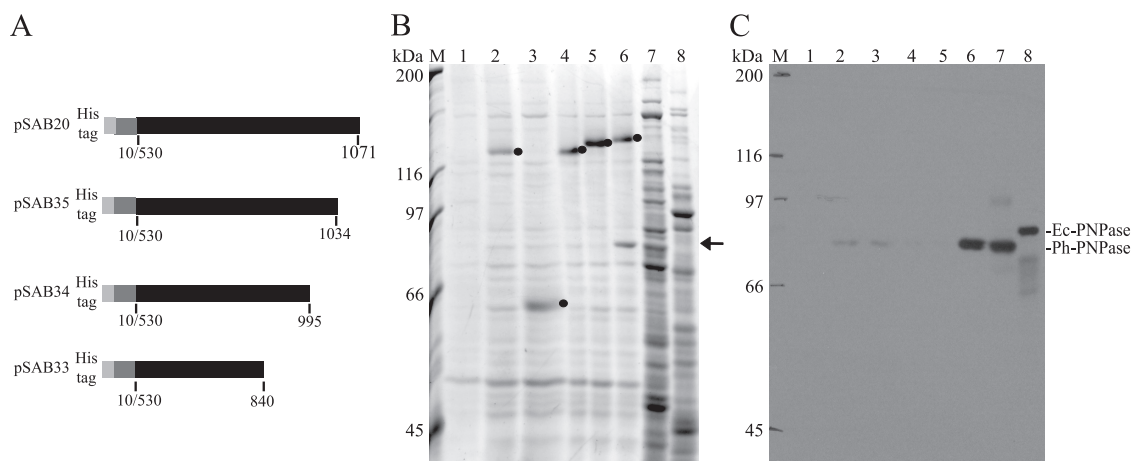


FIG. 7. Interaction between Ph-RNase E and Ph-PNPase. (A) Schematic diagram of His-tagged polypeptides corresponding to the CTH of Ph-RNase E (pSAB20) and a nested set of deletions extending from the C-terminal end (pSAB35, pSAB34, and pSAB33). (B) SDS-PAGE stained with Sypro orange of proteins that copurify with the His-tagged CTH peptides. Lane 1, negative control without His-tagged polypeptide; lane 2, control using the His-tagged CTH of Ec-RNase E; lanes 3 to 6, pSAB33, pSAB34, pSAB35, and pSAB20, respectively; lanes 7 and 8, controls showing *P. haloplanktis* and *E. coli* whole-cell extracts, respectively. M, molecular mass markers. The black dots in lanes 2 to 6 indicate the positions of the His-tagged polypeptides. The arrow to the right of the panel indicates the position of a protein in lane 6 that copurifies with the CTH of Ph-RNase E and migrates at a position corresponding to the molecular mass of Ph-PNPase. (C) Western blot. A gel comparable to the gel shown in panel B was blotted and probed with antibodies against Ec-PNPase. The major signal detected in lane 8 corresponds to Ec-PNPase, which runs as a slightly larger protein than Ph-PNPase (lanes 6 and 7).

washed, and eluted with imidazole. Figure 7B shows SDS-PAGE of the eluates. Lane 1 shows a negative control with a mock reaction that did not contain the CTH, lane 2 shows the result using the Ec-CTH, and lane 6 shows the result using the Ph-CTH. In lane 6, a protein of about 80 kDa copurified with Ph-CTH (indicated by the arrow). Western blotting identified the protein in lane 6 of Fig. 7B as Ph-PNPase (Fig. 7C). In this Western blot, trace amounts of Ph-PNPase were detected in lanes 2 and 3, but this result, which is not reproducible, is likely due to incomplete removal during the wash step. Taken together, these results suggest that the interaction of PNPase and RNase E is species specific. This conclusion is supported by the *in vivo* results shown in Fig. 5, in which we failed to detect an interaction between Ec-PNPase and Ph-RNase E. Each of the deletions (Fig. 7B, lanes 3 to 5) failed to interact with Ph-PNPase, demonstrating that residues 1035 to 1071 of Ph-RNase E are necessary for the interaction with Ph-PNPase. In subsequent work, we overexpressed Ph-PNPase at 25°C in an *E. coli* strain in which the gene encoding Ec-PNPase was disrupted, and we prepared a highly enriched fraction of Ph-PNPase by high-speed centrifugation and ammonium sulfate precipitation. For unknown reasons, we have not been able to demonstrate specific binding to the Ph-CTH using purified Ph-PNPase. Our results therefore need to be interpreted with caution, since we lack proof that Ph-PNPase by itself is sufficient for the interaction with Ph-RNase E.

DISCUSSION

We report here the identification of the RNA degradosome of *P. haloplanktis* and the characterization of microdomains in Ph-RNase E involved in the protein-protein interactions. We have also shown that Ph-RNase E can restore the viability of *E. coli* strains lacking Ec-RNase E. The introduction of the *Ph-rme*

gene on a low-copy-number plasmid (pSAB15) into *E. coli* in which the chromosomal *Ec-rme* gene was disrupted resulted in weak complementation, with detectable colony formation only after 6 days at 25°C. Analysis of Ph-RNase E in this strain showed that the amount was at least 32-fold lower than the normal amount of Ec-RNase E. Thus, the *Ph-rme* gene under endogenous expression signals is poorly expressed in *E. coli*. To improve expression of Ph-RNase E in *E. coli*, we constructed a hybrid gene in which the 5' expression signals of the *Ec-rme* gene were fused to the coding sequence of *Ph-rme*. The resulting fusion on a low-copy-number plasmid (pSAB18) complemented *E. coli* at temperatures ranging from 15 to 37°C. The amount of Ph-RNase E in this strain is about 50% of the normal amount of Ec-RNase E. Taken together, these results show that the poor complementation with the *Ph-rme* gene is due to the low level of Ph-RNase E expression in *E. coli*.

Since Ph-RNase E is obtained from a psychrotolerant bacterium, we were surprised to observe that complementation in *E. coli* at 15°C is weak compared to that of the Ec-RNase E control. We have presented experimental evidence that the amount of Ph-RNase E detected at 15°C is comparable to the amount detected at 30°C. Since the endoribonuclease activity of Ph-RNase E is expected to be comparable to or higher than the activity of Ec-RNase E at 15°C, this result suggests that Ph-RNase E fails to supply a noncatalytic function necessary for growth in the cold. In addition, we have shown that the *E. coli* MC1061 strain harboring the *me131* allele, expressing Ec-RNase E lacking the noncatalytic region (32), grows slower than the parental MC1061 strain at 15°C. These results suggest that the noncatalytic region of Ec-RNase E provides a function that facilitates growth at low temperature. This function could, for example, involve the interaction between Ec-RNase E and a protein component of the RNA degradosome.

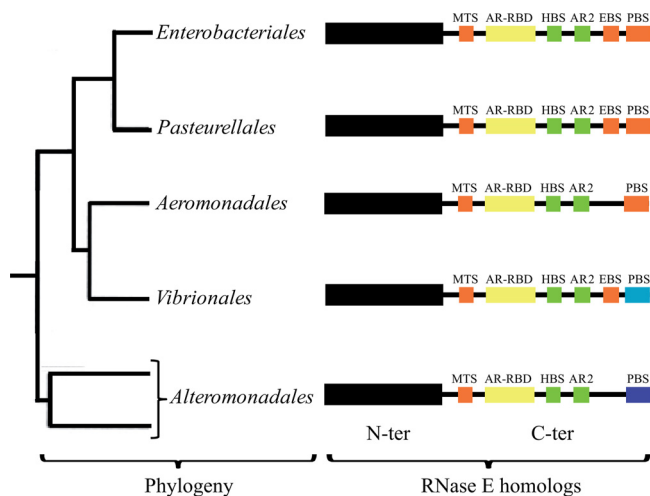


FIG. 8. Primary structure of RNase E homologs in the *Enterobacteriales*, *Pasteurellales*, *Aeromonadales*, *Vibrionales*, and *Alteromonadales*. The tree on the left shows in outline form the relationship of five orders of the *Gammaproteobacteria* (17). The schematic diagrams on the right summarize our understanding of the primary structures of the RNase E homologs of each of these orders. The N-terminal catalytic domain is represented as a black box; the C-terminal noncatalytic region is represented as a line. Microdomains are represented as colored boxes following the scheme described in the legend to Fig. 1. The RNase E homologs of the *Aeromonadales* have a PNPase binding site similar to the homologs from the *Enterobacteriales* and *Pasteurellales* but lack identifiable enolase binding sites based on sequence comparisons. For the RNase E homologs of the *Vibrionales* and *Alteromonadales*, the light and dark blue boxes, respectively, represent PNPase binding sites that are unrelated by sequence to each other or to the corresponding sites in homologs from the *Enterobacteriales* and *Pasteurellales*.

The noncatalytic region of Ec-RNase E contains two well-characterized microdomains that are involved in protein-protein interactions with enolase and PNPase. The structures of these microdomains complexed with their partner proteins have been elucidated by X-ray crystallography. The microdomain involved in enolase binding forms an α -helix that makes an extensive network of hydrogen-bonding interactions at the enolase dimer interface (8). The sequence motif corresponding to the microdomain involved in enolase binding is conserved throughout the *Enterobacteriales*. A recent analysis of *Vibrio angustum* S14, a member of the *Vibrionales*, involving sequence comparisons and two hybrid tests has demonstrated the conservation of the EBS in RNase E homologs of these bacteria (16). Taken together with our results, we can predict that the EBS is conserved in RNase E homologs of the *Enterobacteriales*, *Pasteurellales*, and *Vibrionales* but absent in the *Aeromonadales*, *Alteromonadales*, and more distantly related *Gammaproteobacteria* (Fig. 8). These observations suggest that the interaction with enolase was acquired during the evolution of the *Gammaproteobacteria*. The association of enolase with RNase E in the *Enterobacteriales* could link the mRNA degradation machinery to the control of central intermediary metabolism. *P. haloplanktis* inhabits a marine environment that is poor in sources of carbon, nitrogen, and phosphorus. It notably lacks the cyclic AMP-catabolite gene activator protein (cAMP-CAP) system responsible for catabolite repression and the phosphotransferase system (PTS) required for the transport of

glucose (39). The association of enolase with RNase E in *E. coli* might therefore be an adaptation to a niche such as the animal gut, where nutrient levels vary dramatically and rapid adjustments in the control of nutrient uptake and utilization give a competitive advantage.

The microdomain of Ec-RNase E involved in the protein-protein interaction with Ec-PNPase extends a preexisting β -sheet on the surface of PNPase (43). β -sheet extension has been suggested as a potentially common element in protein-protein interactions (49). The RNase E-PNPase interaction appears to be widespread in the *Proteobacteria*. Our results, however, suggest that the interaction is species specific. That is, Ec-RNase E binds Ec-PNPase but not Ph-PNPase, and Ph-RNase E binds Ph-PNPase but not Ec-PNPase. Our results, together with the recent two-hybrid analysis of the RNase E-PNPase interaction between *Vibrio angustum* S14 homologs (16), shows that this interaction does not correspond to a sequence motif conserved among the *Alteromonadales* or the *Vibrionales*. Since the interaction is species specific, one possibility is that the underlying structural motif for the interaction is different in different bacteria, although this seems unlikely. Another possibility is that the secondary structure involved in β -sheet extension is conserved but that the constraint on protein sequence of the RNase E microdomains involved in β -sheet extension is low. These considerations suggest that the species-specific RNase E-PNPase interaction could involve a conserved β -sheet extension that imposes minimal constraints on the protein sequence.

PNPase is a phosphate-dependent exoribonuclease. Although PNPase has been found to be associated with RNase E in several different bacteria, this is not always the case. Notably, RNase E of the psychrophilic gammaproteobacterium *Pseudomonas syringae* Lz4W has been shown to be associated with RNase R, which is a hydrolytic exoribonuclease (46). Exoribonucleases related to PNPase and RNase R are widely distributed in bacteria, plants, and animals (13, 40). These enzymes represent two distinct families of exoribonucleases. Like *P. haloplanktis*, *Pseudomonas syringae* Lz4W is a cold-adapted marine gammaproteobacterium (50). Since both of these bacteria inhabit similar environmental niches, the formation of an RNA degradosome with a phosphorolytic rather than hydrolytic exoribonuclease does not appear to correlate with the conditions of growth in a cold marine environment.

Our results show that the Ph-RhlB interacts with Ph-RNase E as a component of the RNA degradosome of *P. haloplanktis*. In Ec-RNase E, the minimal binding site for RhlB has been mapped to the region comprising residues 698 to 762 (9), and a sequence motif within the region is well conserved in the *Enterobacteriales* (Fig. 6A). The substitution of a highly conserved arginine residue in this motif for alanine (R730A) abolishes RhlB binding (27). Ph-RNase E contains a related sequence motif in the same region, which includes a conserved arginine residue corresponding to R730. We have shown that deletion of the region corresponding to the motif abolishes the interaction between Ph-RNase E and Ec-RhlB. In Fig. 1C, region 1, corresponding to residues 747 to 758 of Ph-RNase E, is predicted to have the capacity to form secondary structure. We mapped the Ph-HBS to residues 683 to 716. Thus, the region predicted to have the capacity to form secondary structure and the region necessary for binding to RhlB are distinct.

Like other DEAD-box RNA helicases, the catalytic core of RhlB is comprised of two structurally related domains. The second domain of RhlB has been shown to be necessary and sufficient for the interaction with RNase E (9). The surface of RhlB involved in this interaction and the structure of the microdomain corresponding to the binding site in RNase E have not yet been elucidated (see reference 56). The heterologous interaction of Ec-RhlB with Ph-RNase E suggests that the underlying structural motif for the protein-protein interaction is conserved over a large evolutionary distance. Experimental evidence has shown that RhlB needs to interact with RNase E as part of the RNA degradosome to have biological activity (24, 26). The interaction with RNase E activates the ATPase and RNA unwinding activities of RhlB (9, 27, 53, 56). These considerations suggest that the conservation of the RhlB binding site over a large evolutionary distance could be due to structural constraints involved in the control of RhlB activity.

Figure 8 shows a simplified phylogenetic tree of the *Enterobacteriales*, *Pasteurellales*, *Aeromonadales*, *Vibrionales*, and *Alteromonadales* (17) and summarizes our understanding of the primary structure of the RNase E homologs in these orders of the *Gammaproteobacteria*. The identification of the RNA degradosome of *P. haloplanktis* has revealed two widely conserved interactions with RNase E homologs of the *Gammaproteobacteria*. Although the interaction is conserved, the PNPase binding site (PBS) does not correspond to a conserved sequence motif. The light and dark blue boxes for the RNase E homologs of the *Vibrionales* and the *Alteromonadales*, respectively, indicate that the protein sequences of the PBSs are distinct from the sequences in the homologs of the *Enterobacteriales*, *Pasteurellales*, and *Aeromonadales*. The binding site for RhlB (HBS) corresponds to a conserved sequence motif. Despite the lack of overall sequence conservation of the CTH of the RNase E homologs, our result suggests that there is nevertheless a conserved "module" composed of the MTS, AR-RBD, HBS, and AR2. Based on experimental results, we suggested previously that the AR-RBD and AR2 cooperate in the RNA unwinding activity of RhlB (9). The conservation of the MTS/AR-RBD/HBS/AR2 module over a relatively large evolutionary distance suggests an important conserved function, which for example, could be the control of the activity or specificity of RhlB within the RNA degradosome.

ACKNOWLEDGMENTS

We thank I. Bagdiul, M. Dreyfus, and V. Khemici for providing the plasmids and strains; members of the Carpousis group, M. Dreyfus and B. Luisi, for helpful discussions; and B. Clouet-d'Orval and P. Genevaux for critical reading of the manuscript.

S.A.-B. was supported by a predoctoral fellowship from the MESR (Ministère de l'Enseignement Supérieur et de la Recherche). Research in our group is supported by the CNRS (Centre National de la Recherche Scientifique) and the ANR (Agence Nationale de la Recherche, projects CARMa NT05_1-44659 and mRNases BLAN08-1_329396).

REFERENCES

1. Birolo, L., M. L. Tutino, B. Fontanella, C. Gerday, K. Mainolfi, S. Pascarella, G. Sannia, F. Vinci, and G. Marino. 2000. Aspartate aminotransferase from the Antarctic bacterium *Pseudoalteromonas haloplanktis* TAC 125. Cloning, expression, properties, and molecular modelling. *Eur. J. Biochem.* **267**:2790–2802.
2. Callaghan, A. J., J. P. Aurikko, L. L. Ilag, J. Gunter Grossmann, V. Chandran, K. Kuhnel, L. Poljak, A. J. Carpousis, C. V. Robinson, M. F. Symmons,

- and B. F. Luisi. 2004. Studies of the RNA degradosome-organizing domain of the *Escherichia coli* ribonuclease RNase E. *J. Mol. Biol.* **340**:965–979.
3. Callaghan, A. J., M. J. Marcaida, J. A. Stead, K. J. McDowall, W. G. Scott, and B. F. Luisi. 2005. Structure of *Escherichia coli* RNase E catalytic domain and implications for RNA turnover. *Nature* **437**:1187–1191.
4. Carpousis, A. J. 2002. The *Escherichia coli* RNA degradosome: structure, function and relationship to other ribonucleolytic multienzyme complexes. *Biochem. Soc. Trans.* **30**:150–155.
5. Carpousis, A. J., V. Khemici, S. Ait-Bara, and L. Poljak. 2008. Co-immunopurification of multiprotein complexes containing RNA-degrading enzymes. *Methods Enzymol.* **447**:65–82.
6. Carpousis, A. J., B. F. Luisi, and K. J. McDowall. 2009. Endonucleolytic initiation of mRNA decay in *Escherichia coli*. *Prog. Mol. Biol. Transl. Sci.* **85**:91–135.
7. Carpousis, A. J., G. Van Houwe, C. Ehretsmann, and H. M. Krisch. 1994. Copurification of *E. coli* RNase E and PNPase: evidence for a specific association between two enzymes important in RNA processing and degradation. *Cell* **76**:889–900.
8. Chandran, V., and B. F. Luisi. 2006. Recognition of enolase in the *Escherichia coli* RNA degradosome. *J. Mol. Biol.* **358**:8–15.
9. Chandran, V., L. Poljak, N. F. Vanzo, A. Leroy, R. N. Miguel, J. Fernandez-Recio, J. Parkinson, C. Burns, A. J. Carpousis, and B. F. Luisi. 2007. Recognition and cooperation between the ATP-dependent RNA helicase RhlB and ribonuclease RNase E. *J. Mol. Biol.* **367**:113–132.
10. Chenna, R., H. Sugawara, T. Koike, R. Lopez, T. J. Gibson, D. G. Higgins, and J. D. Thompson. 2003. Multiple sequence alignment with the Clustal series of programs. *Nucleic Acids Res.* **31**:3497–3500.
11. Clamp, M., J. Cuff, S. M. Searle, and G. J. Barton. 2004. The Jalview Java alignment editor. *Bioinformatics* **20**:426–427.
12. Coburn, G. A., and G. A. Mackie. 1999. Degradation of mRNA in *Escherichia coli*: an old problem with some new twists. *Prog. Nucleic Acid Res. Mol. Biol.* **62**:55–108.
13. Condon, C., and H. Putzer. 2002. The phylogenetic distribution of bacterial ribonucleases. *Nucleic Acids Res.* **30**:5339–5346.
14. Deutscher, M. P. 2006. Degradation of RNA in bacteria: comparison of mRNA and stable RNA. *Nucleic Acids Res.* **34**:659–666.
15. Duilio, A., S. Madonna, M. L. Tutino, M. Pirozzi, G. Sannia, and G. Marino. 2004. Promoters from a cold-adapted bacterium: definition of a consensus motif and molecular characterization of UP regulative elements. *Extremophiles* **8**:125–132.
16. Erce, M. A., J. K. Low, P. E. March, M. R. Wilkins, and K. M. Takayama. 2009. Identification and functional analysis of RNase E of *Vibrio angustum* S14 and two-hybrid analysis of its interaction partners. *Biochim. Biophys. Acta* **1794**:1107–1114.
17. Gao, B., R. Mohan, and R. S. Gupta. 2009. Phylogenomics and protein signatures elucidating the evolutionary relationships among the *Gammaproteobacteria*. *Int. J. Syst. Evol. Microbiol.* **59**:234–247.
18. Gao, J., K. Lee, M. Zhao, J. Qiu, X. Zhan, A. Saxena, C. J. Moore, S. N. Cohen, and G. Georgiou. 2006. Differential modulation of *E. coli* mRNA abundance by inhibitory proteins that alter the composition of the degradosome. *Mol. Microbiol.* **61**:394–406.
19. Grunberg-Manago, M. 1999. Messenger RNA stability and its role in control of gene expression in bacteria and phages. *Annu. Rev. Genet.* **33**:193–227.
20. Jager, S., O. Fuhrmann, C. Heck, M. Hebermehl, E. Schiltz, R. Rauhut, and G. Klug. 2001. An mRNA degrading complex in *Rhodobacter capsulatus*. *Nucleic Acids Res.* **29**:4581–4588.
21. Jager, S., M. Hebermehl, E. Schiltz, and G. Klug. 2004. Composition and activity of the *Rhodobacter capsulatus* degradosome vary under different oxygen concentrations. *J. Mol. Microbiol. Biotechnol.* **7**:148–154.
22. Jain, C., and J. G. Belasco. 1995. RNase E autoregulates its synthesis by controlling the degradation rate of its own mRNA in *Escherichia coli*: unusual sensitivity of the *rne* transcript to RNase E activity. *Genes Dev.* **9**:84–96.
23. Kaberdin, V. R., A. Miczak, J. S. Jakobsen, S. Lin-Chao, K. J. McDowall, and A. von Gabain. 1998. The endoribonucleolytic N-terminal half of *Escherichia coli* RNase E is evolutionarily conserved in *Synechocystis* sp. and other bacteria but not the C-terminal half, which is sufficient for degradosome assembly. *Proc. Natl. Acad. Sci. U. S. A.* **95**:11637–11642.
24. Khemici, V., and A. J. Carpousis. 2004. The RNA degradosome and poly(A) polymerase of *Escherichia coli* are required *in vivo* for the degradation of small mRNA decay intermediates containing REP-stabilizers. *Mol. Microbiol.* **51**:777–790.
25. Khemici, V., L. Poljak, B. F. Luisi, and A. J. Carpousis. 2008. The RNase E of *Escherichia coli* is a membrane-binding protein. *Mol. Microbiol.* **70**:799–813.
26. Khemici, V., L. Poljak, I. Toesca, and A. J. Carpousis. 2005. Evidence *in vivo* that the DEAD-box RNA helicase RhlB facilitates the degradation of ribosome-free mRNA by RNase E. *Proc. Natl. Acad. Sci. U. S. A.* **102**:6913–6918.
27. Khemici, V., I. Toesca, L. Poljak, N. F. Vanzo, and A. J. Carpousis. 2004. The RNase E of *Escherichia coli* has at least two binding sites for DEAD-box

- RNA helicases: functional replacement of RhlB by RhlE. *Mol. Microbiol.* **54**:1422–1430.
28. **Kushner, S. R.** 2002. mRNA decay in *Escherichia coli* comes of age. *J. Bacteriol.* **184**:4658–4665.
 29. **Lee, K., J. A. Bernstein, and S. N. Cohen.** 2002. RNase G complementation of rne null mutation identifies functional interrelationships with RNase E in *Escherichia coli*. *Mol. Microbiol.* **43**:1445–1456.
 30. **Lee, K., X. Zhan, J. Gao, J. Qiu, Y. Feng, R. Meganathan, S. N. Cohen, and G. Georgiou.** 2003. A *Streptomyces coelicolor* functional orthologue of *Escherichia coli* RNase E shows shuffling of catalytic and PNPase-binding domains. *Mol. Microbiol.* **48**:349–360.
 31. **Lee, K., X. Zhan, J. Gao, J. Qiu, Y. Feng, R. Meganathan, S. N. Cohen, and G. Georgiou.** 2003. RraA: a protein inhibitor of RNase E activity that globally modulates RNA abundance in *E. coli*. *Cell* **114**:623–634.
 32. **Leroy, A., N. F. Vanzo, S. Sousa, M. Dreyfus, and A. J. Carpousis.** 2002. Function in *Escherichia coli* of the non-catalytic part of RNase E: role in the degradation of ribosome-free mRNA. *Mol. Microbiol.* **45**:1231–1243.
 33. **Li, X., P. Romero, M. Rani, A. K. Dunker, and Z. Obradovic.** 1999. Predicting protein disorder for N-, C-, and internal regions. *Genome Inform. Ser. Workshop Genome Inform.* **10**:30–40.
 34. **Li, Z., S. Pandit, and M. P. Deutscher.** 1999. RNase G (CafA protein) and RNase E are both required for the 5' maturation of 16S ribosomal RNA. *EMBO J.* **18**:2878–2885.
 35. **Lopez, P. J., I. Marchand, S. A. Joyce, and M. Dreyfus.** 1999. The C-terminal half of RNase E, which organizes the *Escherichia coli* degradosome, participates in mRNA degradation but not rRNA processing *in vivo*. *Mol. Microbiol.* **33**:188–199.
 36. **Mackie, G. A.** 1998. Ribonuclease E is a 5'-end-dependent endonuclease. *Nature* **395**:720–723.
 37. **Marcaida, M. J., M. A. DePristo, V. Chandran, A. J. Carpousis, and B. F. Luisi.** 2006. The RNA degradosome: life in the fast lane of adaptive molecular evolution. *Trends Biochem. Sci.* **31**:359–365.
 38. **McDowall, K. J., and S. N. Cohen.** 1996. The N-terminal domain of the rne gene product has RNase E activity and is non-overlapping with the arginine-rich RNA-binding site. *J. Mol. Biol.* **255**:349–355.
 39. **Medigue, C., E. Krin, G. Pascal, V. Barbe, A. Bernsel, P. N. Bertin, F. Cheung, S. Cruveiller, S. D'Amico, A. Duilio, G. Fang, G. Feller, C. Ho, S. Mangenot, G. Marino, J. Nilsson, E. Parrilli, E. P. Rocha, Z. Rouy, A. Sekowska, M. L. Tutino, D. Vallenet, G. von Heijne, and A. Danchin.** 2005. Coping with cold: the genome of the versatile marine Antarctica bacterium *Pseudoalteromonas haloplanktis* TAC125. *Genome Res.* **15**:1325–1335.
 40. **Mian, I. S.** 1997. Comparative sequence analysis of ribonucleases HII, III, II PH and D. *Nucleic Acids Res.* **25**:3187–3195.
 41. **Miczak, A., V. R. Kabardin, C. L. Wei, and S. Lin-Chao.** 1996. Proteins associated with RNase E in a multicomponent ribonucleolytic complex. *Proc. Natl. Acad. Sci. U. S. A.* **93**:3865–3869.
 42. **Morita, T., K. Maki, and H. Aiba.** 2005. RNase E-based ribonucleoprotein complexes: mechanical basis of mRNA destabilization mediated by bacterial noncoding RNAs. *Genes Dev.* **19**:2176–2186.
 43. **Nurmohamed, S., B. Vaidialingam, A. J. Callaghan, and B. F. Luisi.** 2009. Crystal structure of *Escherichia coli* polynucleotide phosphorylase core bound to RNase E, RNA and manganese: implications for catalytic mechanism and RNA degradosome assembly. *J. Mol. Biol.* **389**:17–33.
 44. **Ow, M. C., Q. Liu, and S. R. Kushner.** 2000. Analysis of mRNA decay and rRNA processing in *Escherichia coli* in the absence of RNase E-based degradosome assembly. *Mol. Microbiol.* **38**:854–866.
 45. **Prud'homme-Genereux, A., R. K. Beran, I. Iost, C. S. Ramey, G. A. Mackie, and R. W. Simons.** 2004. Physical and functional interactions among RNase E, polynucleotide phosphorylase and the cold-shock protein, CsdA: evidence for a 'cold shock degradosome.' *Mol. Microbiol.* **54**:1409–1421.
 46. **Purusharth, R. I., F. Klein, S. Sulthana, S. Jager, M. V. Jagannadham, E. Evguenieva-Hackenberg, M. K. Ray, and G. Klug.** 2005. Exoribonuclease R interacts with endoribonuclease E and an RNA helicase in the psychrotrophic bacterium *Pseudomonas syringae* Lz4W. *J. Biol. Chem.* **280**:14572–14578.
 47. **Py, B., C. F. Higgins, H. M. Krisch, and A. J. Carpousis.** 1996. A DEAD-box RNA helicase in the *Escherichia coli* RNA degradosome. *Nature* **381**:169–172.
 48. **Regonesi, M. E., M. Del Favero, F. Basilico, F. Briani, L. Benazzi, P. Tortora, P. Mauri, and G. Deho.** 2006. Analysis of the *Escherichia coli* RNA degradosome composition by a proteomic approach. *Biochimie* **88**:151–161.
 49. **Remaut, H., and G. Waksman.** 2006. Protein-protein interaction through beta-strand addition. *Trends Biochem. Sci.* **31**:436–444.
 50. **Shivaji, S., N. S. Rao, L. Saisree, V. Sheth, G. S. Reddy, and P. M. Bhargava.** 1989. Isolation and identification of *Pseudomonas* spp. from Schirmacher Oasis, Antarctica. *Appl. Environ. Microbiol.* **55**:767–770.
 51. **Taraseviciene, L., G. R. Bjork, and B. E. Uhlin.** 1995. Evidence for an RNA binding region in the *Escherichia coli* processing endoribonuclease RNase E. *J. Biol. Chem.* **270**:26391–26398.
 52. **Tock, M. R., A. P. Walsh, G. Carroll, and K. J. McDowall.** 2000. The CafA protein required for the 5'-maturation of 16S rRNA is a 5'-end-dependent ribonuclease that has context-dependent broad sequence specificity. *J. Biol. Chem.* **275**:8726–8732.
 53. **Vanzo, N. F., Y. S. Li, B. Py, E. Blum, C. F. Higgins, L. C. Raynal, H. M. Krisch, and A. J. Carpousis.** 1998. Ribonuclease E organizes the protein interactions in the *Escherichia coli* RNA degradosome. *Genes Dev.* **12**:2770–2781.
 54. **Wachi, M., G. Umitsuki, M. Shimizu, A. Takada, and K. Nagai.** 1999. *Escherichia coli* cafA gene encodes a novel RNase, designated as RNase G, involved in processing of the 5' end of 16S rRNA. *Biochem. Biophys. Res. Commun.* **259**:483–488.
 55. **Worrall, J. A., M. Gorna, N. T. Crump, L. G. Phillips, A. C. Tuck, A. J. Price, V. N. Bavro, and B. F. Luisi.** 2008. Reconstitution and analysis of the multienzyme *Escherichia coli* RNA degradosome. *J. Mol. Biol.* **382**:870–883.
 56. **Worrall, J. A., F. S. Howe, A. R. McKay, C. V. Robinson, and B. F. Luisi.** 2008. Allosteric activation of the ATPase activity of the *Escherichia coli* RhlB RNA helicase. *J. Biol. Chem.* **283**:5567–5576.